



CHORUS

This is the accepted manuscript made available via CHORUS. The article has been published as:

Facilitated diffusion of proteins through crumpled fractal DNA globules

Jan Smrek and Alexander Y. Grosberg

Phys. Rev. E **92**, 012702 — Published 1 July 2015

DOI: [10.1103/PhysRevE.92.012702](https://doi.org/10.1103/PhysRevE.92.012702)

Facilitated diffusion of proteins through crumpled fractal DNA globule

Jan Smrek* and Alexander Y. Grosberg
*Center for Soft Matter Research and Department of Physics,
New York University, New York, NY 10003, USA*

We explore how does the specific fractal globule conformation, found for the chromatin fiber of higher eukaryotes and topologically constrained dense polymers, affect the facilitated diffusion of proteins in this environment. Using scaling arguments and supporting Monte Carlo simulations we relate DNA looping probability distribution, fractal dimension and protein non-specific affinity for the DNA to the effective diffusion parameters of the proteins. We explicitly consider correlations between subsequent re-adsorption events of the proteins and find that facilitated diffusion is faster for the crumpled globule conformation with high intersegmental surface dimension, than in the case of dense fractal conformations with smooth surfaces. As a by-product we obtain expression for macroscopic conductivity of a hypothetical material consisting of conducting fractal nanowires immersed in a weakly conducting medium.

I. INTRODUCTION

Facilitated diffusion of proteins such as transcription factors in the cell has been invoked as a possible likely mechanism speeding up the passive diffusive finding of specific target sites on DNA [1–3]. The facilitated diffusion consists of repeated tours of three-dimensional diffusion in the nuclear space interrupted by non-specific adsorption of the protein to the DNA, subsequent one dimensional diffusional sliding along the DNA, followed by desorption and another diffusion in the free space etc. While the sliding along the DNA reduces the dimensionality of the searched space, the three dimensional tours break the correlation between visited sites and prevent repetitive visits of the same DNA sites. In this way, the facilitated diffusion mechanism can explain low values of measured search time for proteins that are for certain biological conditions and DNA conformations, significantly below search times predicted in the absence of the one-dimensional diffusion tours.

In principle, the effectiveness of facilitated diffusion depends on DNA conformation. Indeed, after a three dimensional tour whether the protein re-adsorbs on a previously “scanned” DNA segment or on an uncorrelated one, depends on how are the DNA segments folded in space [4]. So far, most of the studies in this area considered DNA as a straight rod or an assembly of several such rods or did not consider the conformation explicitly [2, 5–7]. This simplification is somewhat justified by the fact that 1D sliding length is usually quite small, on the order of or smaller than DNA persistence length as found in prokaryotes and in vitro [8–10]. Nevertheless, it is of significant interest to understand also facilitated diffusion for other DNA arrangements. In this regard, two prototypical conformations, that of Gaussian coil and of equilibrium globule were examined in [11, 12]. Recently, it became clear that the third broad class of conformations is of interest, that of crumpled or fractal globules, which

is found in long eukaryotic DNA and topologically constrained polymer systems [13, 14]. The goal of this work is to consider a model of facilitated diffusion through a crumpled globule. Let us note that the facilitated diffusion in a generic fractal characterized by fractal and walk dimensions was examined in [15] where the distribution of first passage time was calculated. However, that work did not consider correlations between subsequent adsorptions which play a central role of the present work and as we show have an effect on the diffusion properties. Moreover, it is not clear how is the walk dimension related to the conformational properties of the chromatin fiber. Therefore, we relate the diffusion properties to the directly accessible conformational properties of crumpled globule reflected in its fractal dimension and contact probability.

Let us briefly summarize the crumpled globule conformational properties, that are available from experiments on DNA, such as Hi-C method [16, 17], and from simulations of long topologically constrained polymers [18, 19]. Above the entanglement length L_e , estimated in [14] for the DNA and discussed here later, the probability of two DNA loci to be in close proximity in space decreases with their distance along the DNA contour as a power-law with the exponent $-\gamma$ close to -1 from below (e.g. -1.08 human, -1.05 mouse). Moreover, it was found that the DNA conformation is self-similar and compact that is manifested by the scaling of the mean end-to-end distance or gyration radius of a segment with its length $R_g(s) \sim s^\nu$ with exponent $\nu = 1/d = 1/3$. Interestingly, these conformational properties reflected in exponents ν and γ seem to be universal across different higher organisms and cell types and therefore it is very interesting to explore their functional consequences.

However, we have to emphasize that most presently studied transcription factors perform their search on the scale smaller than the onset of the fractal globule conformation as discussed also in section V. Nevertheless, besides the theoretical interest of the present problem, in principle one can design an artificial experiment to overcome this limitation and probe the fractal DNA conformation by means of measuring the facilitated diffusion.

* js5013@nyu.edu

To quantify the search process with facilitated diffusion in fractal globule, we employ a number of rather strong simplifications. Firstly, the polymer conformation is assumed to be immobile during the whole search process. It has been observed that the chromatin *in vivo* is subject not only to the thermal fluctuations, but also ATP-dependent directed movements. The resulting dynamics exhibits subdiffusive behaviour on short time and length scales as well as correlated large scale motions on the scale of tens of seconds that is comparable to the protein search times [20]. Hence the effect of dynamics is relevant, however a proper hydrodynamic description is only beginning to emerge [21] and it is reasonable to understand the conformational implications at first and account for dynamics in future work. Secondly, although the DNA occupies only about 1% of the volume of the nucleus [14] the presence of histone proteins and other nuclear bodies can raise this value significantly and act as crowding agents. This can have an effect on the DNA density distribution that has been studied in this context in [22] and that we assume to be homogeneous. Moreover, the motion of particles in concentrated polymer solutions and equilibrium globule conformation even without affinity to the polymer matrix can be subdiffusive on small scales or significantly hindered due to excluded volume effects [23–26]. However, in [27] it was shown that some types of nuclear proteins indeed overcome such “barriers” and can slide along the DNA fiber, although with smaller diffusion coefficient. Additionally, it was shown also *in vivo* that the environment is highly penetrable by the proteins despite the high density [28]. We take the possible crowding effects into account only implicitly, by taking the diffusion coefficients along the DNA and in the “free” space as parameters of the problem and investigate their impact on the search rate. To quantify realistically the protein search process in the eukaryotic interphase nucleus one should relax these simplifications. However to judge their relative relevance the natural first step is to understand their individual implications. Our present work aims to be such a step in the case of the large scale DNA conformation.

Our model for the DNA conformation is based on the fractal space-filling curves, that have been shown to mimic the chromatin fiber conformation properties above the entanglement length (see also different approach [29]). By construction they are self-similar and the space-filling property is reflected in the scaling of the gyration radius with length with the exponent $\nu = 1/3$ as for the DNA. It was shown [14] that the exponent γ governing the scaling of the contact probability, is related to the fractal dimension d_b of the surface of the volume occupied by the space-filling curve, by the relation $2 - \gamma = d_b/d = \beta$. While the classical space-filling curves such as Hilbert curve [30] have smooth surfaces with $\beta = 2/3$, the DNA contact probability scaling is reproduced by space-filling curves with d_b close to 3 or in other words β close to unity (from below) [31]. It is precisely the effect of the exponent β on the search pro-

cess and protein dynamics in the nucleus that we want to capture.

In the next section we present scaling arguments for the specific binding rate of the proteins to their targets as a function of the protein affinity for the DNA, diffusional properties and the exponent β . Then we calculate effective diffusion coefficient governing the transport of the protein through the fractal medium of nucleus using the analogy with electric transport properties. In the subsequent section we present the various regimes for the binding rates resulting from relations between various lengthscales of the problem and we compare our findings with numerical simulations.

II. THE MODEL

Our approach follows that of Hu et. al. [11] who find the lengthscale of uncorrelated protein readsorption from the balance of 3D and 1D transport, however we employ important modifications regarding the DNA conformation.

We consider the chromatin fiber of length L and diameter b to occupy a volume v representing the nucleus. For simplicity all the microscopic lengthscales such as the protein size, chromatin fiber diameter, and target size are taken to be of the same order b . The volume fraction of the chromatin Lb^2/v is assumed low enough so the protein can diffuse freely in between the DNA with a diffusion coefficient D_3 . The protein can nonspecifically adsorb to the DNA with energy ε and the corresponding Boltzmann parameter $y = e^{\varepsilon/kT}$ that is assumed to be independent of the DNA sequence. Although some proteins can bind to more than one strand at a time, we do not assume such complication here. When the protein is adsorbed it can diffuse along the fiber with a diffusion coefficient D_1 .

We assume there is just a single target on the whole DNA and we are interested in the mean first passage time of a protein to the target, averaged over the initial protein position relative to the target location. As the DNA is immobile one can use a standard technique to calculate the mean first passage time. We can imagine there is a sink of proteins at the target and when a protein reaches the target it is introduced back to the system at random location. Then, there is an average constant flux J to the target and the average target binding time is just given by the inverse of this flux $\tau = 1/J$. We do not assume any effects due to internal degrees of freedom of the protein [32] or imperfect target recognition efficiency.

Naturally, the binding rate J is proportional to the total protein concentration c , as long as the proteins do not interact with each other, which we assume as well. If there was no nonspecific adsorption of the proteins to the DNA, the rate of hitting the target by a pure 3D diffusion is given by a Smoluchowski rate $J_s = 4\pi D_3 cb$, which is a steady state solution to an absorbing sphere of size b . In what follows we drop the factor of 4π in

J_s as we do also with all other numerical factors in our scaling arguments. We will present the results in form of J/J_s to show the speed-up or slowdown of the facilitated diffusion with respect to the pure 3D case.

The main reason for a possible speed-up of the facilitated diffusion is that the sliding along the DNA effectively increases the target size. Due to 1D sliding, the protein reaches the target even if it adsorbs onto the DNA within some contour distance λ from the target. The lengthscale λ , called antenna length, governs the extent of correlated readsorption hence is the crossover length between 1D and 3D diffusion. In other words the protein moves on average distance λ by 1D diffusion while the transport to the antenna is governed by 3D diffusion (see illustrative fig. 1). Naively, one could consider λ to be equal to the average sliding length, which can be estimated as $l_{\text{slide}} \sim b(yD_1/D_3)^{1/2}$ [9, 11] (the protein spends adsorbed time $t \sim b^2y/D_3$, during which it covers distance $(D_1t)^{1/2}$). However in general λ can be longer than l_{slide} because of the correlated readsorption: protein explores segment of length l_{slide} and desorbs, then performs a short 3D diffusion tour and adsorbs again on a correlated place e.g. such that was visited in the previous sliding. Then the protein slides again along the DNA distance l_{slide} , which however does not completely overlap with the previously visited segment. Repeating such correlated tours, the (the antenna) length explored before the protein readsorbs on a completely uncorrelated location can be greater than the pure sliding length (see also [11] for more detailed explanation). Such a correlated readsorption does not change the sliding time significantly and this can be estimated as λ^2/D_1 . To see this, one has to realize that after desorption, the protein is very close to the DNA and therefore, with probability close to unity it adsorbs back on the DNA before diffusing far away. Such a short diffusion event lasts a microscopic time at most of the order of b^2/D_3 . As one can easily check, this is smaller than the time of 1D diffusion between two protein desorptions l_{slide}^2/D_1 and therefore the sliding time including correlated readsorptions is dominated by the 1D diffusion estimate above. Then the delivery rate of proteins to the target through the 1D diffusion is given by $J = J_1 = c_{\text{ads}}\lambda/(\lambda^2/D_1)$, where c_{ads} is the concentration of adsorbed proteins. So far, the antenna length is yet to be determined from a balance between the one-dimensional and three-dimensional transport. That is, in steady state the flux J_1 of proteins to the target sink is to be compensated by a 3D flux J_3 of proteins delivered to the antenna.

The main improvement of the present work from the earlier approach [11] is the rate J_3 that is to be adjusted for the specific fractal conformation consistent with that of the eukaryotic DNA. As we neglect the density fluctuations of the DNA, the mean distance r traveled by a protein before encountering the DNA, scales as $r \sim (v/L)^{1/2}$. This is in fact, in the scaling sense, the same as the penetration length of a random walker into a mesh of cylinders of radius $b \ll r$ and mean density $1/r^3$. To see that, one

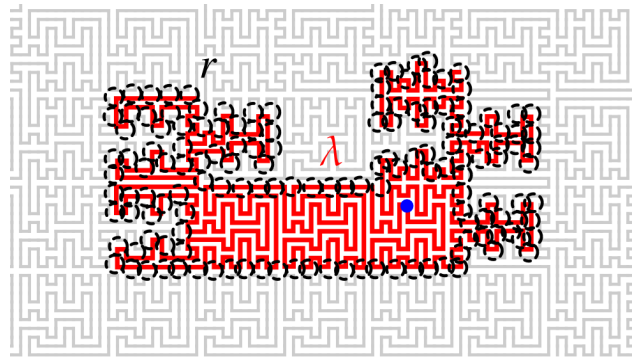


FIG. 1. (Color online) Simplistic view of the antenna following a space-filling curve in 2D. Antenna (thick red line) of length λ around the target (filled blue circle) follows a space-filling curve (thin grey) representing the DNA conformation. The black dashed empty circle of radius r represent the scale of free diffusion in between the DNA strands. Collection of the r circles in the figure depicts the accessible surface of the antenna by the free diffusion.

can express the distance traveled by a random walker before hitting a cylinder as $(D_3\tau_{Sc})^{1/2}$, where τ_{Sc} is Smoluchowski time to hit a cylinder of radius b and length r . Solving for the corresponding steady state, one can see that $\tau_{Sc} \sim (D_3c_w r)^{-1}$, where we dropped all numerical and also logarithmic factors and where c_w is the concentration of walkers i.e. $1/r^3$. That means, the average traveled distance of a random walker is up to a numerical factor the same as the mean interchain distance r . At first, for simplicity we will assume that $r \sim p \sim L_e$, where p is the persistence length which means that the chromatin fiber is straight below the scale r and behaves as space-filling curve with some β above r . We make this artificial assumption to concentrate on the effect of the large-scale structural properties of the DNA on the binding rate, however later in section IV we will relax this assumption to show what is the impact of conformation on the smaller scales. As the 3D diffusion takes place only on or below lengthscale r , in order for the protein to be delivered to the antenna, it has to hit one of the DNA cylinders of length r covering the accessible surface of the antenna (fig. 1). As we assume $\lambda > r$ i.e. is above the fractal threshold, the number of these cylinders scales as $(\lambda/r)^\beta$ [31]. Then the rate J_3 is $(\lambda/g)^\beta$ times the delivery rate to one such cylinder which is $D_3c_{\text{free}}r$.

The balance of the $J_1 = J_3$

$$D_1 \frac{c_{\text{ads}}}{\lambda} = D_3 c_{\text{free}} r \left(\frac{\lambda}{r} \right)^\beta \quad (1)$$

gives us λ in terms of c_{free} and c_{ads} that can be further simplified by the following consideration. On the way to the target the proteins experience many adsorption and desorption events hence we can consider the adsorbed and free proteins to be in equilibrium and write for the respective concentration

$$c_{\text{ads}}/c_{\text{free}}b^2 = y, \quad (2)$$

where we assumed the adsorbed proteins are confined within a distance b of the DNA. Then we can express the antenna length as

$$\lambda \sim (\delta y b^2 r^{\beta-1})^{1/(1+\beta)}, \quad (3)$$

where we defined $\delta = D_1/D_3$. To get the target binding rate we have to plug this back into J_1 (or equivalently to J_3). The result will depend on the values of c_{ads} and c_{free} of course, which can however be evaluated exactly using the fact that the total concentration of proteins is fixed. The total number of proteins satisfies

$$cv = c_{\text{ads}}Lb^2 + c_{\text{free}}(v - Lb^2) \quad (4)$$

and we can express the concentrations as function of the parameters:

$$c_{\text{ads}} \simeq \frac{c y b^2}{y L b^2 + v} \sim \begin{cases} c y b^2 & \text{if } y \ll v/Lb^2 = (r/b)^2 \\ c v/L & \text{if } y \gg (r/b)^2 \end{cases} \quad (5)$$

$$c_{\text{free}} \simeq \frac{c v}{y L b^2 + v} \sim \begin{cases} c & \text{if } y \ll (r/b)^2 \\ c v/Lb^2 y & \text{if } y \gg (r/b)^2 \end{cases} \quad (6)$$

The upper expressions of (5) and (6) we call a 'weak adsorption' (WA) regime and the lower correspond to 'strong adsorption' (SA) regime. Using these relations the binding rate in the different regimes, using (1) and (3), is given by

$$\frac{J}{J_S} \sim \begin{cases} (\delta y)^{\beta/(1+\beta)} (r/b)^{(1-\beta)/(1+\beta)} & \text{if WA} \\ \delta^{\beta/(1+\beta)} y^{-1/(1+\beta)} (r/b)^{(3+\beta)/(1+\beta)} & \text{if SA} \end{cases} \quad (7)$$

As noted before the expression for J_3 in (1) holds only if $\lambda \gg r$, hence using (3) we have to check if this is satisfied. The condition gives $y \gg (r/b)^2/\delta$ which means the weak adsorption regime ($y \ll (r/b)^2$) can only exist in the form of the upper line of (7) if $\delta \gg 1$. If that is the case one can see that with increasing protein affinity the binding rate increases at first as $y^{\beta/(1+\beta)}$ until y reaches about $(r/b)^2$ and then starts to decrease more rapidly as $y^{-1/(1+\beta)}$. The initial increase is due to the higher D_1 , which makes the transport of the proteins faster along the DNA on scales below λ than the three dimensional diffusion and as y grows, more proteins are adsorbed which increases the binding rate. However as y increases beyond $(r/b)^2$, λ grows as well and the reciprocal character of the 1D diffusion starts to dominate over the speedup due to $\delta > 1$ and the overall binding rate decreases.

As mentioned above β varies in the range $[2/3, 1]$, where the lower values correspond to smooth Hilbert-like curves (\mathcal{HC}) while values close to 1 are for space-filling curves with very wiggly surfaces (\mathcal{SC}) similar in statistical properties to the DNA. As β increases the uncorrelated readsorption is more likely as the surface of the visited segment of the fiber has deep protrusions of other - uncorrelated segments. That is why λ is decreasing

function of β and J/J_S grows more rapidly and for large y decreases less rapidly for \mathcal{SC} than for \mathcal{HC} . However the obtained dependence of λ and subsequently of J on β is rather weak. The increase of J with y in WA regime has exponent $\beta/(1+\beta)$ that gives range $[2/5, 1/2]$ and the decrease of J with y is governed by exponent $-1/(1+\beta)$ in range $[-3/5, -1/2]$.

III. EFFECTIVE DIFFUSION COEFFICIENT - NANOWIRES ANALOGY

Experimentally more accessible than the specific binding rate, might be the effective diffusion coefficient D_{eff} that governs the transport of proteins on large scales. For example one can design an experiment with diffusing particles that exhibit only nonspecific adsorption or choose a DNA that does not contain specific targets for the given protein. In that case the fractal properties of the DNA conformation translate in the effective diffusion coefficient. Although we can calculate this quantity directly from the previous considerations, in what follows we use the analogy with electrical conductivity of a hypothetical composite material as it is instructive to present other facet of the same problem and the area of applicability of the present theory.

The material consists of nanowires with conductivity σ_1 in the particular fractal conformation of the DNA, that are immersed in a medium with conductivity σ_3 . Our aim is to calculate the macroscopic conductivity σ_{eff} of the material as this is related to the D_{eff} of our diffusion problem as explained in detail in [33]. To make this work self-contained let us briefly summarize the main idea of this correspondence. We assume there is no target in the system, but we look for an effective transport coefficient when a constant gradient of (chemical) potential is applied. In the steady state the current density j of both, the electric current and the diffusion satisfy $\vec{\nabla} \cdot \vec{j} = 0$. The electric current density is subject to Ohm's law $\vec{j} = -\sigma(\vec{r})\vec{\nabla}\phi$ and the diffusion current can be expressed using the Smoluchowski equation as $\vec{j} = -D(\vec{r})c(\vec{r})\vec{\nabla}[\ln c(\vec{r}) - \varepsilon(\vec{r})/kT]$. In general the parameters of the two problems the conductivity σ , the diffusion coefficients D , the protein concentration c and the nonspecific adsorption energy ε are spatially dependent. In a tube of radius b along the DNA the diffusion coefficient is D_1 , protein concentration c_{ads}/b^2 and the adsorption energy is ε , while elsewhere the quantities have values D_3 , c_{free} and zero respectively. Similarly, the nanowires of thickness b have the conformation of the DNA and their conductivity is equal to σ_1 , while the conductivity of the medium around is σ_3 . Then the mapping between the two problems can be easily expressed by the following dictionary: $\sigma_1 \leftrightarrow D_1 c_{\text{ads}}/b^2$ and $\sigma_3 \leftrightarrow D_3 c_{\text{free}}$ which can be written using the equilibrium condition (2) as

$$\sigma_1/\sigma_3 \leftrightarrow \delta y, \quad (8)$$

where $\delta = D_1/D_3$ as before. To relate the macroscopic transport coefficients, one writes the Ohm's law in terms of σ_{eff} and Smoluchowski equation with D_{eff} and c , which results in

$$\sigma_{\text{eff}}/\sigma_3 \leftrightarrow D_{\text{eff}}c/D_3c_{\text{free}} \quad (9)$$

where the ratio c/c_{free} is 1 in weak adsorption regime or $y(b/r)^2$ in strong adsorption by equation (6).

As in the diffusion problem, there is lengthscale λ characterizing the length over which the current flows mostly in the wires, before it crosses through the medium to another uncorrelated piece of wire. The main idea is to express the macroscopic conductivity in terms of this lengthscale and then find λ maximizing the conductivity. The reason behind this approach is the minimal dissipation principle, that has been showed to be equivalent to Kirchhoff's laws if the linear (Ohm's) law is considered for the the material constituents [34].

We consider a piece of the material that is the size of λ in 3D space as the conductivity at this scale is about the same as the macroscopic one, because the correlation effects are on and below this scale. As mentioned above, we assume that λ follows the fractal space-filling scaling of the wire (DNA), that is, it's spatial size, such as gyration radius, scales as $(\lambda/r)^{1/d}$ where $d = 3$ is the space dimension. That means the resistance of a cube of this size is about $R \sim (\sigma_{\text{eff}}r(\lambda/r)^{1/d})^{-1}$. This overall resistance consists of the resistance due to the wire and resistance due to the medium. The wire contributes the resistance λ/σ_1b^2 that is connected in series with a group of parallel connected bridges each of which has resistance $1/r\sigma_3$ as the flow through the medium is on lengthscale r . The number of these bridges scales with the surface of the wire, that goes as $(\lambda/r)^\beta$ so the total resistance of the cube satisfies

$$\frac{1}{\sigma_{\text{eff}}r(\lambda/r)^{1/d}} \simeq \frac{\lambda}{\sigma_1b^2} + \frac{1}{\sigma_3r(\lambda/r)^\beta}. \quad (10)$$

We maximize the σ_{eff} as function of λ , or equivalently, minimize the resistance and we find

$$\lambda \sim (\sigma_1b^2/\sigma_3r^{1-\beta})^{1/(1+\beta)} \quad (11)$$

which is, using the dictionary (8), the same as λ in the search process given by equation (3). This is not surprising as the Kirchhoff's laws, as a consequence of the minimum dissipation, require the same current to flow through the two serial components, which is the same as equating the two particle fluxes in the diffusion problem as was done in (1). Then the effective conductivity is given by

$$\sigma_{\text{eff}} \sim \sigma_3 \left[\frac{\sigma_1 b^2}{\sigma_3 r^2} \right]^{(\beta-1/d)/(1+\beta)} \quad (12)$$

Using the dictionaries (8), (9) and the concentration relation (2), one finds for the effective diffusion coefficient

in the two regimes

$$\frac{D_{\text{eff}}}{D_3} \sim [\delta(b/r)^2]^{\frac{\beta-1/d}{1+\beta}} \begin{cases} y^{(\beta-1/d)/(1+\beta)} & \text{if WA} \\ y^{-(1+1/d)/(1+\beta)} & \text{if SA} \end{cases} \quad (13)$$

In the weak adsorption regime the effective diffusion coefficient increases very slowly with the adsorption strength y , with exponent $1/5$ for \mathcal{HC} and faster, with exponent $1/3$ for \mathcal{SC} with β close to one. Interestingly, in the strong adsorption regime the effective diffusion coefficient decreases more rapidly with y for \mathcal{HC} with exponent $-4/5$, while for the DNA-like conformations one gets exponent $-2/3$. These findings can be rationalized in the following sense. As discussed above, $y > (r/b)^2/\delta$ to satisfy $\lambda > r$ and for weak adsorption regime to exist, δ must be greater than unity, in which case $D_{\text{eff}} > D_3$ and the non-specific binding improves the effective transport of proteins by diffusion of proteins through the system of "fast highways" (although very winding) of the DNA. This can be checked by calculating time to travel λ along the DNA and compare it with time to diffuse $r(\lambda/r)^{1/d}$ by 3D diffusion. The speedup however is more pronounced for the \mathcal{SC} than for \mathcal{HC} because the recursive character of 1D diffusion is broken more often in the case of \mathcal{SC} as is manifested by shorter λ . In the strong adsorption regime most of the proteins are adsorbed and following the DNA conformation. The less often the uncorrelated re-adsorption happens the more time-consuming this sliding is, hence the transport over Hilbert curve is less efficient than for wiggly surface curves.

The target binding rate calculated in the previous section can be understood also using the effective diffusion coefficient. One expects that the target binding rate is $J \sim D_{\text{eff}}cr(\lambda/r)^{1/d}$ i.e. it is the Smoluchowski rate with the effective diffusion coefficient and target size equal to the 3D size of the antenna $r(\lambda/r)^{1/d}$. This is indeed the case for the weak adsorption as one can easily check using equations (13) and (3), however one has to be more careful in the strong adsorption regime. In the SA regime, most of the proteins are adsorbed, hence the apparent concentration hitting the target is that of c_{ads} . That is there are $c_{\text{ads}}r$ proteins in the volume of cylinder of radius b and length r , hence the apparent concentration is $c_{\text{ads}}r/rb^2 = c(r/b)^2$, where the last equality holds in SA by equation (5). Taking this into account, the binding rate is $J \sim D_{\text{eff}}c(r^2/b^2)r(\lambda/r)^{1/d}$, with diffusion coefficient from bottom line of (13), which agrees exactly with the binding rate of the strong regime - bottom line of equation (7).

To test these ideas we simulated facilitated diffusion on a cubic lattice in an environment with a space-filling curve and measured the effective diffusion coefficient D_{eff} as function of the parameters. We used two types of space-filling curves: (i) Hilbert curve (\mathcal{HC}) of sixth iteration with $\beta = 2/3$ and (ii) second iteration of the curve with fractal surface (\mathcal{SC}) from [31] with $\beta = 0.89$. Both of these curves, in their original construction, have length 64^3 lattice sites, but to allow for free diffusion in the space between the curves we use three times finer lattice for dif-

fusion. This means the curves are of length $L = 3 \times 64^3$ and homogeneously occupy volume $v = (3 \times 64)^3$ i.e. 1/9 of all the (finer) lattice sites, or in other words $b = 1$ and $r = 3$ in the lattice units. We checked numerically, also for other occupation fraction, that the mean traveled distance by free 3D diffusion is indeed about r as calculated above. To measure D_{eff} we set the particle, that occupies one lattice site, to diffuse in a periodic array of such volumes v , each with the curve of length L . If the particle is on the site occupied by the curve it performs a random walk along the curve and at each step there is a probability π , to perform a jump off the curve to the free space where it diffuses with diffusion coefficient D_3 until it hits the curve again. The probability π is controlled by the adsorption strength y by $\pi = (2 + y)^{-1}$, where the constant 2 is due to twice as many ways to jump off the curve than to stay on it (in cubic lattice).

In figure 2 we plot D_{eff} as function of y for $\delta = 1$, which means there is only strong adsorption regime where $y \sim \pi^{-1}$. For $y > 10$ the values of D_{eff} start to differ as $\lambda > r$ and the correlation effects start to play a role resulting in stronger decrease of the D_{eff} for the Hilbert curve. The theoretical prediction of the slope of graphs

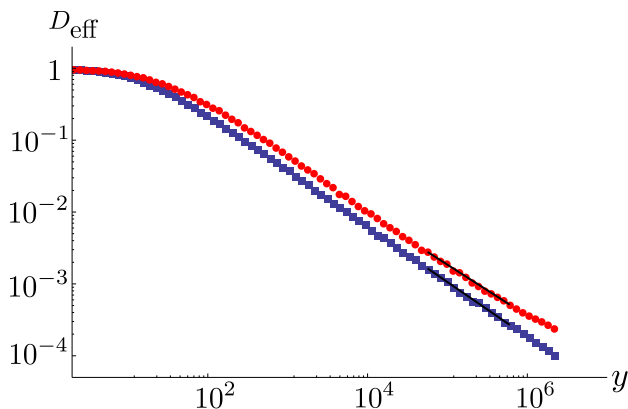


FIG. 2. (Color online) Effective diffusion coefficient D_{eff} as function of adsorption strength y for the Hilbert curve (blue squares) and space-filling curve with $\beta = 0.89$ (red circles) in loglog scale (errorbars smaller than symbols used) for $\delta = 1$. Black lines are best fits in large y range (see text), with slope -0.76 ± 0.01 for Hilbert curve and -0.71 ± 0.01 for the curve with wiggly surface. Each data point represents diffusion coefficient extracted from the mean square displacement of a very long (facilitated) random walks averaged over 5×10^6 realizations.

for large y in fig. 2 is $-(1 + 1/d)/(1 + \beta)$ from eq. (13), which is -0.8 for \mathcal{HC} and -0.7 for \mathcal{SC} . To capture correctly the slopes of the strong adsorption regime, λ has to be sufficiently large to be insensitive to the discrete nature of the fractal. The construction of the \mathcal{SC} is based on a segment that is 512 monomers long, therefore we want λ to be at least of the same order. Hence we fit values of D_{eff} for $y > 4 \times 10^4$, which corresponds to $\lambda > 100r$. This is not an issue for the Hilbert curve that is based on a segment of length 8 monomers. On the

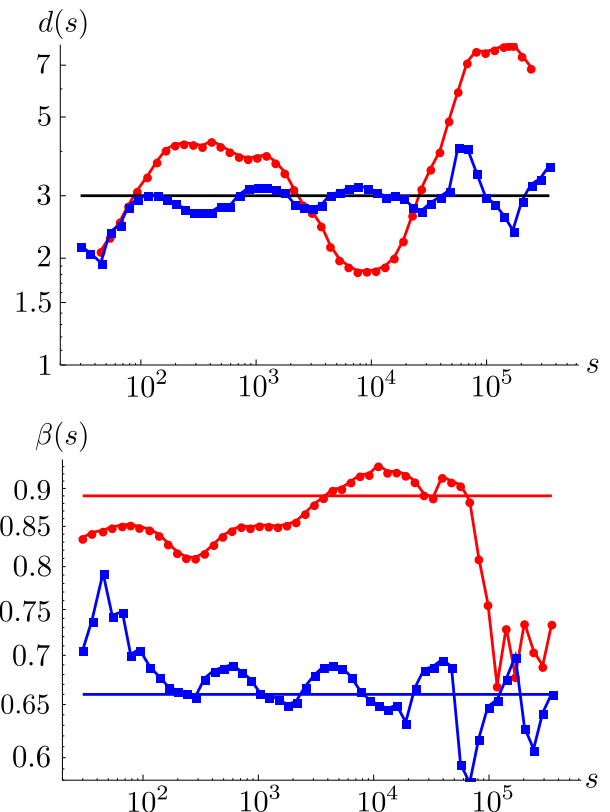


FIG. 3. (Color online) Top: Fluctuations of the fractal dimension d of the Hilbert curve (blue squares) and the wiggly curve (red circles) average dimension is $d = 3$ in both cases marked with black straight line. Bottom: Fluctuations of the exponent β , average values are marked by the straight lines $2/3$ for the Hilbert curve, 0.89 for the wiggly curve. Statistics of fluctuations of the exponents d and β have large errors for long segments s , due to small sampling ensemble.

other hand as both curves are of finite size, we have to keep $y < L/b \simeq 5 \times 10^5$, so that the particle does not feel the ends of the DNA during the 1D diffusion (as might be visible by the decrease of slope of the D_{eff} for large y in fig. 2 in the case of \mathcal{SC}). Therefore to fit the slopes we take $4 \times 10^4 < y < L/b$ as shown in fig. 2 by black lines. Although the predictions match with the fitted values (fig. 2) reasonably (-0.8 vs -0.76 and -0.7 vs 0.71), varying the range of y one gets values of the exponents for Hilbert curve in the range $[-0.78, -0.75]$ and for the wiggly curve in range $[-0.7, -0.74]$. We believe the reason for this discrepancy can be in the fluctuations of the exponent values β and d of the curves (fig. 3), that are inherent to the iterative curve construction as explained in [31]. The effective fractal dimension $d(s)$ corresponding to lengthscale s has been calculated as the exponent of the gyration radius of a segment of length s averaged over positions in the curve. The segment lengths were chosen to be $s_k = 3 * 1.2^k$, $k \in [10, 63]$ and the exponent $d(s)$ was obtained from the slope of the loglog plot from seven data points surrounding the given lengthscale s ,

which corresponds to lengthscale range roughly $[s/2, 2s]$. The variation of $\beta(s)$ was obtained in the same way, measured as the scaling exponent of the number of surface monomers. Naturally, the greater the range of s we take, the smaller the fluctuations are. If the complete range $[b, L]$ is taken for \mathcal{HC} and \mathcal{SC} at these finite iterations, the exponents agree with their theoretical values (marked in fig. 3).

Similarly to $D_{\text{eff}}(y)$, in fig. 4 we measured the dependence of the effective diffusion coefficient on $\delta = D_1/D_3$. Here the predicted exponent $(\beta - 1/d)/(1 + \beta)$ is independent on the regime, and is 0.2 for the \mathcal{HC} and 0.29 for the \mathcal{SC} .

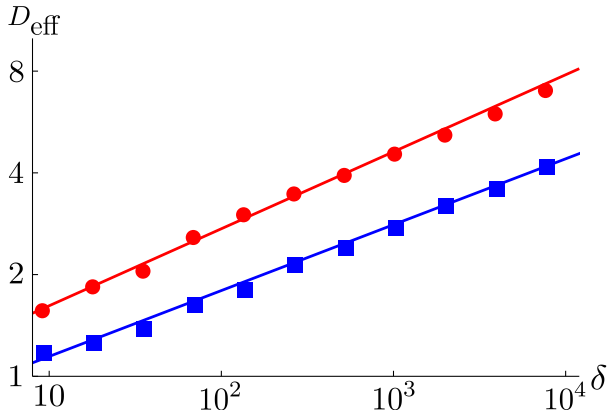


FIG. 4. (Color online) Effective diffusion coefficient D_{eff} as function of ratio $\delta = D_1/D_3$ for the Hilbert curve (blue squares) and space-filling curve with $\beta = 0.89$ (red circles) in loglog scale for $\pi = 0.16$ i.e. $y \simeq 4$. Lines are best fits, with slope 0.19 for Hilbert curve and 0.23 ± 0.01 for the curve with wiggly surface. Each data point represents diffusion coefficient extracted from the mean square displacement of a very long (facilitated) random walks averaged over 2.5×10^7 realizations.

Considering the fluctuations of β and d we should not expect a perfect match of the numerics with the theory that considers only mean values of the exponents, only if the simulations were performed over even wider ranges of parameters provided longer (higher iteration) curves were available. However we believe the numerics supports the theory as (i) D_{eff} for the Hilbert curve is always lower than the one for wiggly curve (ii) the exponents for the \mathcal{HC} are in any range of parameters lower than those for \mathcal{SC} as predicted by the theory and (iii) the values of the exponents are at least in the correct ballpark predicted by the theory.

IV. OTHER LENGTHSCALES

So far we have discussed the effect of the large scale space-filling organization on the protein binding rate and effective transport coefficient. As mentioned above these effects start to play a role if the 1D sliding diffusion covers

lengths larger than the onset of the fractal conformation L_e . To complement the study, we briefly mention the possible binding rate and effective diffusion coefficient regimes at lower scales computed in [11, 33]. To do so, we have to employ the relations between the monomer size b , persistence length of the DNA fiber p , the entanglement length L_e and the corresponding spatial size $r_e \sim (pL_e)^{1/2}$ and the lengthscale r . While the monomer size of the *fiber* is on the scale of a few nanometers, the persistence length of the DNA fiber is estimated to be around 150 nm [35]. The entanglement length L_e can be from 100 nm to around 1.1 μm , but most likely close to 300 nm, while the spatial size r is on the scale of 100 nm (see Tables 1 and 2. in [14]). Based on these relations, we will consider $p \sim r$, which means the chromatin fiber is straight below r . Above r the fiber either follows the space-filling fractal conformation if $r \sim L_e$ as considered in previous section, or if $L_e \gg r$, there is a window of an equilibrium globule conformation above r and below L_e , that can be described as a network of mesh size r , where each individual chain follows random walk statistics (Flory theorem).

Let us briefly describe the possible regimes of binding rate summarized in the table I and figure 5, based on the relation between the antenna length and other length-scales. If the antenna is shorter than r , it is straight and is equal to the sliding distance $b(\delta y)^{1/2}$. The overall binding rate depends on adsorption strength - grows with $y^{1/2}$ in WA and decreases in SA. Interestingly, these results hold even if λ is longer than r and still shorter than L_e . The reason for this is that the DNA fiber conformation follows a random walk which is not compact enough to shield itself and this way provide correlated readsorption due to the presence of other - uncorrelated strands in distance r from the fiber. Therefore, any part of the antenna in this regime is accessible by 3D diffusion from distance r and the results for binding rate of “straight mesh” from [11] apply (shown as regimes A and B in tab. I and fig. 5). These are effectively the same as our previous results with $\beta = 1$ (any monomer is accessible from nearby chains), however the effective diffusion coefficient is different as the DNA is not a space-filling fractal on this scale. Based on protein adsorption there are again two regimes, where now the weak adsorption regime exists only if $\delta > 1$, to satisfy $\lambda > r$.

If λ gets longer than the entanglement length one has to adjust the lengthscales in the preceding section by $r \rightarrow L_e$ in equations (1) and (3), which have an effect on prefactors involving r/b , however the general dependence on y and δ remains the same. In fact, this substitution is not completely trivial as the 3D delivery to the antenna takes place on the scale r . In order to deliver the proteins to a piece of size L_e , one can deliver it to any of the L_e/r sites of length r . However as the antenna is much longer than L_e , not all of the λ/L_e pieces are accessible, but only $(\lambda/L_e)^\beta$ of them - those that lie on the surface of the fractal conformation. Therefore the 3D delivery rate is $J_3 \sim D_3 c_{\text{free}} r(L_e/r)(\lambda/L_e)^\beta$ which effectively is the

same as the suggested substitution $r \rightarrow L_e$. These are regimes C and D in tab. I and fig. 5

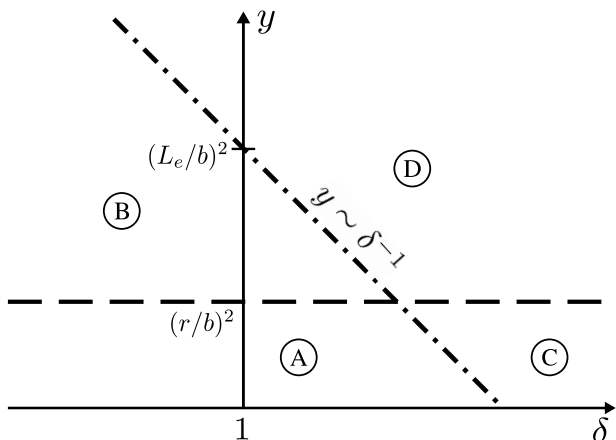


FIG. 5. Phase diagram of binding rate in loglog scale. The dashed line $y = (r/b)^2$ delimits the adsorption strength: weak adsorption below and strong adsorption above. Dot-dashed line proportional to δ^{-1} delimits regimes corresponding to space-filling conformation of antenna (above) and that of straight antenna or antenna following random walk in the mesh of other chains (below). The values of antenna lengths and corresponding binding rates are summarized in Table I.

Similarly one can investigate effective diffusion coefficient for lengthscales below L_e . This has been done in [33], so in Table II and Figure 6 we just summarize the results in the present notation using the dictionaries (8) and (9). There are two important facts to be noted. First, the binding rate in these regimes where $\lambda > r$ can not be calculated simply as Smoluchowski rate with effective diffusion coefficient and target size proportional to size of λ , as it was demonstrated in the case of the space-filling antenna. This is because the antenna follows a random walk which is not compact and therefore, delivery of protein to the sphere of size $r_e \sim (r\lambda)^{1/2}$ does not necessarily guarantee the hitting of the target as there are still many uncorrelated chains in such a sphere. Second fact, related to the first one, is that the effective diffusion coefficient is different for case $\lambda < r$ and $\lambda > r$ in contrast to J which depends only on the adsorption strength in this two cases.

Regimes A1 and A2 (tab. II and fig. 6) represent the cases when $\lambda < r$, which means the effective diffusion coefficient is dominated by D_3 and in the strong adsorption regime is even reduced due to the adsorbed proteins. In regimes B1 and B2, $\lambda > r$ hence follows a random walk. Regimes C and D (in tab. II and fig. 6) represent the antenna in a space-filling curve conformation. To account for $L_e > r$ in these regimes, one has to modify equation (12) for the overall resistance. The left hand side must be replaced by $(\sigma_{\text{eff}} r_e (\lambda/L_e)^{1/d})^{-1}$ to properly account the spatial size of the antenna, where $r_e \sim (rL_e)^{1/2}$ is the size of entanglement blob and there are λ/L_e of these blobs per antenna. Additionally, on the right hand side of (12), r should be replaced by L_e as explained above

for the binding rate case. Note that these changes do not affect the expression for λ from Table I and result in the effective coefficient showed in Table II.

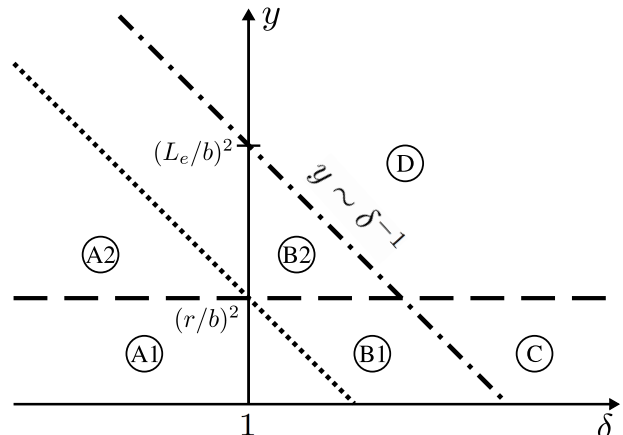


FIG. 6. Phase diagram of effective diffusion coefficient in loglog scale. The dashed line $y = (r/b)^2$ delimits the adsorption strength: weak adsorption below and strong adsorption above. Dotted and dot-dashed lines are proportional to δ^{-1} . Dotted lines delimits regimes of $\lambda > r$ (above) and $\lambda < r$ (below), while dot-dashed line delimits the space-filling conformation of antenna (above) and that of antenna following random walk in the mesh of other chains (below). The values of antenna lengths and corresponding D_{eff} are summarized in Table II.

V. DISCUSSION AND CONCLUSIONS

The fact that the space-filling fractal structure of the chromatin fiber is present on scales larger than 150 nm poses a severe restriction on the applicability of our results for the search process in vivo. In order for these structural effects to play role, δ or y has to be large enough so that the sliding length $b(y\delta)^{1/2}$ is greater than L_e . While the value of D_3 is known to be around $0.1 - 1 \mu\text{m}^2\text{s}^{-1}$ [1, 28] for transcription factors, the value of D_1 is more difficult to measure and can be more susceptible to the protein details and ionic strength. However, using single molecules techniques D_1 was measured for some prokaryotic proteins [36, 37], but also for eukaryotes [27] and the values fall in range $10^{-4} - 10^{-1} \mu\text{m}^2\text{s}^{-1}$. The resulting values of δ are in general smaller than unity and fall in range in $[10^{-4}, 1]$, most likely somewhat closer to the upper bound (around 0.1) under physiological conditions in eukaryotes as shown in [27]. The latter work is particularly illuminating as it demonstrated that the 1D diffusion along DNA is present for some proteins with $D_1 \simeq 0.03 \mu\text{m}^2\text{s}^{-1}$ even if the DNA is decorated by nucleosomes. Considering the value of $\delta \simeq 0.1$ one can estimate that in order to observe effects related to the space-filling conformations, the nonspecific adsorption energy must be $\varepsilon \simeq 8 - 12kT$, which is relatively high, but possible in principle. In this estimate we assumed that the

Regime	Description	λ	J/J_s
A	weak adsorption, $\lambda < L_e$	$b(\delta y)^{1/2}$	$(\delta y)^{1/2}$
B	strong adsorption, $\lambda < L_e$		$(r/b)^2(\delta/y)^{1/2}$
C	weak adsorption, $\lambda > L_e$	$(\delta y b^2 L_e^{\beta-1})^{1/(1+\beta)}$	$(\delta y)^{\beta/(1+\beta)} (L_e/b)^{(1-\beta)/(1+\beta)}$
D	strong adsorption, $\lambda > L_e$		$(\delta^\beta/y)^{1/(1+\beta)} (L_e^{1-\beta} r^2/b^{3-\beta})^{1/(1+\beta)}$

TABLE I. Summary of binding rates and antenna lengths in regimes defined by adsorption strength and relation between lengthscale. Boundaries of regimes *A-D* are depicted in Figure 5.

Regime	Description	λ	D_{eff}/D_3
A1	weak adsorption, $\lambda < r < L_e$	$b(\delta y)^{1/2}$	1
A2	strong adsorption, $\lambda < r < L_e$		$(r/b)^2/y$
B1	weak adsorption, $r < \lambda < L_e$		$(b/r)(\delta y)^{1/2}$
B2	strong adsorption, $r < \lambda < L_e$		$(r/b)(\delta/y)^{1/2}$
C	weak adsorption, $\lambda > L_e$	$(\delta y b^2 L_e^{\beta-1})^{1/(1+\beta)}$	$(\delta y b^2/L_e^2)^{(\beta-1/d)/(1+\beta)} L_e/r_e$
D	strong adsorption, $\lambda > L_e$		$(\delta b^2/L_e^2)^{(\beta-1/d)/(1+\beta)} y^{-(1+1/d)/(1+\beta)} L_e/r_e$

TABLE II. Summary of effective diffusion coefficients and antenna lengths in regimes defined by adsorption strength and relation between lengthscales. Boundaries of regimes *A-D* are depicted in Figure 6. In regimes A1,A2,B1 and B2, values of D_{eff}/D_3 are adapted from [33].

protein slides along the chromatin fiber and not following all the details of the DNA chain wrapped around the histones. This is reasonable assumption also supported by the experimental evidence in [27], but brings an issue of the efficiency of the specific site recognition. Taking this into account would decrease the binding rate by a factor of order 10, calculated as the ratio of the linear density of bare DNA to that of the DNA fiber [14], however the different scaling regimes should remain the same.

The chromatin dynamics that we do not take into consideration can have an impact on the correlated readsorption. Some approaches such as [12] for coiled DNA, assume the DNA conformation fluctuates sufficiently quickly to consider subsequent relocations as independent. Although this is likely to be good approximations on small lengthscales, on larger scales the chromatin dynamics in vivo exhibits large correlated motions [20], which means the local environment of a sufficiently long segment does not necessarily change rapidly. Therefore we hypothesize that the correlated readsorption might play a role in the search process. As the nature of the dynamic territories is not yet understood a natural first step is to consider the static picture that we presented in here and postpone the dynamic aspect for future work.

Let us also mention that the maximal binding rate is obtained on the crossover between weak and strong adsorption in any of the regimes. Interestingly conformations with higher β (hence smaller γ) provide the greatest acceleration and smallest deceleration due to enhanced possibility of uncorrelated readsorption. Moreover, the binding rates dependence on y and δ for conformations with β close to unity are very similar to those for equi-

librium globule conformation which is characteristic for lower organisms such as prokaryotes or yeast.

To conclude, we presented a scaling theory for the impact of correlated readsorption on the specific target binding rate and effective diffusion coefficient in case of the space-filling fractal conformation found in higher eukaryotes. We showed how does these quantities depend on protein diffusion properties, nonspecific affinity for the DNA and most importantly exponent $\gamma = 2 - \beta$ characterizing the DNA conformation obtained from HiC experiments. Such considerations should in principle be used to indirectly probe the DNA conformation by measurements of effective diffusion coefficient as function of the affinity tunable by salt concentration. As a by-product we obtained effective conductivity of a material composed of conducting nanowires immersed in a medium with different conductivity. Such a hypothetical material could in principle be realized from a melt of polymer nano-rings that on large scales have similar space-filling fractal properties with high β as the eukaryotic DNA.

To develop the protein search theory, we have adopted many simplifying assumptions, such as the static DNA conformation, no viscoelastic effects or crowding restrictions for the protein diffusion, single specific binding site and no exponent fluctuations. Indeed, it would be very interesting to relax these simplifications, especially the dynamic aspect, and investigate their impact on the diffusion process. The present simplified picture aims at connecting structure to function by bridging the two so far disconnected lines of research - DNA fractal globule conformation in nucleus and facilitated diffusion of protein search process.

[1] M. Sheinman, O. Bènichou, Y. Kafri, and R. Voituriez, Rep. Prog. Phys. **75**, 026601 (2012).

[2] O. G. Berg, R. B. Winter, and P. H. Von Hippel, Bio-

- chemistry **20**, 6929 (1981).
- [3] P. H. von Hippel and O. G. Berg, *J. Biol. Chem.* **264**, 675 (1989).
- [4] R. K. Das and A. B. Kolomeisky, *Phys. Chem. Chem. Phys.* **12**, 2999 (2010).
- [5] M. Coppey, O. Bénichou, R. Voituriez, and M. Moreau, *Biophys. J.* **87**, 1640 (2004).
- [6] R. F. Bruinsma, *Physica A* **313**, 211 (2002).
- [7] M. Slutsky and L. A. Mirny, *Biophys. J.* **87**, 4021 (2004).
- [8] P. Hammar, P. Leroy, A. Mahmutovic, E. G. Marklund, O. G. Berg, and J. Elf, *Science* **336**, 1595 (2012).
- [9] S. E. Halford and J. F. Marko, *Nucleic Acids Res.* **32**, 3040 (2004).
- [10] A. Mahmutovic, O. G. Berg, and J. Elf, *Nucleic Acids Research*(2015).
- [11] T. Hu, A. Y. Grosberg, and B. Shklovskii, *Biophys. J.* **90**, 2731 (2006).
- [12] M. A. Lomholt, B. van den Broek, S.-M. J. Kalisch, G. J. L. Wuite, and R. Metzler, *Proc. Natl. Acad. Sci.* **106**, 8204 (2009).
- [13] L. A. Mirny, *Chromosome Res.* **19**, 37 (2011).
- [14] J. Halverson, J. Smrek, K. Kremer, and A. Grosberg, *Rep. Prog. Phys.* **77**, 022601 (2014).
- [15] O. Bénichou, C. Chevalier, B. Meyer, and R. Voituriez, *Phys. Rev. Lett.* **106**, 038102 (2011).
- [16] E. de Wit and W. de Laat, *Gene. Dev.* **26**, 11 (2012).
- [17] E. Lieberman-Aiden, N. L. van Berkum, L. Williams, M. Imakaev, T. Ragozcy, A. Telling, I. Amit, B. R. Lajoie, P. J. Sabo, M. O. Dorschner, R. Sandstrom, B. Bernstein, M. A. Bender, M. Groudine, A. Gnirke, J. Stamatoyannopoulos, L. A. Mirny, E. S. Lander, and J. Dekker, *Science* **326**, 289 (2009).
- [18] J. D. Halverson, W. B. Lee, G. S. Grest, A. Y. Grosberg, and K. Kremer, *J. Chem. Phys.* **134**, 204904 (2011).
- [19] M. Imakaev, K. Tchourine, S. K. Nechaev, and L. Mirny, *Soft Matter*(2014).
- [20] A. Zidovska, D. A. Weitz, and T. J. Mitchison, *Proc. Natl. Acad. Sci.* **110**, 15555 (2013).
- [21] R. Bruinsma, A. Grosberg, Y. Rabin, and A. Zidovska, *Biophys. J.* **106**, 1871 (2014).
- [22] S. A. Isaacson, C. A. Larabell, M. A. Le Gros, D. M. McQueen, and C. S. Peskin, *B. Math. Biol.* **75**, 2093 (2013).
- [23] D. S. Banks and C. Fradin, *Biophys. J.* **89**, 2960.
- [24] C. C. Fritsch and J. Langowski, *J. Chem. Phys.* **133**, 025101 (2010).
- [25] J. Halverson, “Diffusion of particles in the melt of rings,” (2014), private communication.
- [26] A. Bancaud, S. Huet, N. Daigle, J. Mozziconacci, J. Beaudouin, and J. Ellenberg, *EMBO J.* **28**, 3785 (2009).
- [27] J. Gorman, A. J. Pys, M.-L. Visnapuu, E. Alani, and E. C. Greene, *Nat. Struct. Mol. Biol.* **17**, 932 (2010).
- [28] R. D. Phair and T. Misteli, *Nature* **404**, 604 (2000).
- [29] G. Bunin and M. Kardar, *ArXiv e-prints*.
- [30] D. Hilbert, *Math. Ann.* **38**, 459 (1891).
- [31] J. Smrek and A. Y. Grosberg, *Physica A* **392**, 6375 (2013).
- [32] L. Hu, A. Y. Grosberg, and R. Bruinsma, *Biophys. J.* **95** (2008).
- [33] T. Hu, A. Y. Grosberg, and B. I. Shklovskii, *Phys. Rev. B* **73**, 155434 (Apr 2006).
- [34] I. Prigogine, *Introduction to thermodynamics of irreversible processes*, (Interscience Publishers, New York, 1967).
- [35] J. Dekker and B. van Steensel, in *Handbook of Systems Biology: Concepts and Insights*, edited by M. Walhout, M. Vidal, and J. Dekker (Elsevier, 2013) Chap. 7, pp. 137–151.
- [36] Y. Wang, R. Austin, and E. Cox, *Phys. Rev. Lett.* **97**, 048302 (Jul 2006).
- [37] J. Elf, G.-W. Li, and X. S. Xie, *Science* **316**, 1191 (2007).